ChemComm

Catalytic NH3 Oxidation to N2 by Hydrogen Atom Abstraction using a Low-valent Molybdenum Complex

Journal:	*ChemComm*
Manuscript ID	CC-COM-04-2025-002433.R1
Article Type:	Communication

SCHOLARONE™
Manuscripts

Please do not adjust margins

ChemComm

COMMUNICATION

Catalytic NH_3 Oxidation to N_2 by Hydrogen Atom Abstraction using a Low-valent Molybdenum Complex

Received 00th January 2025,
Accepted 00th January 2025

DOI: 10.1039/x0xx00000x

www.rsc.org/

Rory J. Benedict,[a] Zachariah M. Heiden,[b] David N. Stephens,[a] Navamoney Arulsamy,[c] and Michael T. Mock[a,*]

The complexes *fac*-[(CO)$_3$Mo($P_2^{tBu}N_2^{Ph}$)(L)] (L = NCCH$_3$, NH$_3$) catalyze NH_3 oxidation to N_2 using phenoxyl radicals as H atom acceptors. Using the sterically bulky trityl- substituted phenoxyl radical generated up to 88 equiv N_2 per Mo.

Ammonia (NH_3) is a promising alternative to carbon-based fuels due to its high energy density, and established means of storage and transportation.[1] The widespread adoption of NH_3 as a practical, large-scale, alternative fuel will require environmentally conscious processes for NH_3 production that minimize CO_2 emissions.[2] NH_3 can be utilized in NH_3 fuel cells,[3] or as a H_2 carrier[4] in the catalytic decomposition of NH_3 into H_2 and N_2, further underscoring NH_3 as a versatile energy vector for a range of applications.

Molecular complexes utilizing transition metals or main-group elements have been used to activate the strong N–H bonds of NH_3, and several molecular catalysts have been reported employing chemo- and electrocatalytic approaches to convert NH_3 to N_2 or hydrazine (N_2H_4).[5] To date, catalytic NH_3 oxidation catalysts used only five metals: Mn,[6] Fe,[7] Ni,[8] Cu,[9] Ru[10]; with Ru as the predominant metal over the past six years. Collectively, these reports have led to a greater understanding of the broad range of factors controlling N–H bond activation and N–N bond forming mechanisms en route to N_2 formation.

While numerous molybdenum complexes catalyze N_2 reduction to generate NH_3,[11] a Mo-based NH_3 oxidation catalyst has not been reported. However, Mo has been shown to activate the N–H bonds of NH_3,[12] and mediate the critical N–N bond forming steps relevant to catalytic NH_3 oxidation to N_2.[13] Transition metal complexes containing *fac*-coordinated carbonyl ligands are an established structure type for small molecule activation and catalysis.[14] We postulated a tricarbonyl Mo(0) complex bearing a $P^R{}_2N^R{}_2$ ligand[15] i.e. *fac*-[(CO)$_3$Mo($P^{tBu}{}_2N^{Ph}{}_2$)(L)] (L = NCCH$_3$ (**1**), NH$_3$ (**2**)) could catalyze NH_3 oxidation using organic radicals as H atom acceptors.[10b, 12a, 16] Herein we report the synthesis, characterization, and catalytic NH_3 oxidation to N_2 via hydrogen atom abstraction (HAA) under ambient conditions using complexes **1** and **2**.

Heating a solution of Mo(CO)$_3$(CHT) (CHT = cycloheptatriene) and $P^{tBu}{}_2N^{Ph}{}_2$ in a 1:1 mixture of acetonitrile and fluorobenzene (PhF) at 80 °C for 72 h afforded **1** as a tan solid in 20% isolated yield, Fig. 1 (panel a). **1** exhibits a singlet at 36.9 ppm in the ^{31}P NMR spectrum. Treatment of **1** with an atmosphere of NH_3 or $^{15}NH_3$ in PhF formed *fac*-[(CO)$_3$Mo($P^{tBu}{}_2N^{Ph}{}_2$)(NH$_3$)] (**2** or **2^{15N}**), isolated as a light yellow microcrystalline solid in 84% yield, Fig. 1 (panel a). **2^{15N}** exhibits a singlet at 32.6 ppm in the ^{31}P NMR spectrum, while the ^{1}H NMR spectrum showed a doublet of triplets at 2.0 ppm ($J_{15N\text{-}H}$ = 67.1 and $J_{31P\text{-}H}$ 3.0 Hz) for the $^{15}NH_3$ ligand. This assignment was further corroborated by a cross-peak in the ^{1}H-^{15}N HSQC spectrum corresponding to a ^{15}N chemical shift at −424.6 ppm (vs. NO_2CH_3). Notably, **2** is stable in vacuum toward NH_3 loss.

The molecular structures of **1** and **2** were determined by single crystal X-ray diffraction. Each complex exhibits a distorted octahedral geometry of the Mo centre consisting of a *fac* arrangement of the three carbonyls, the chelating $P^{tBu}{}_2N^{Ph}{}_2$, and acetonitrile (in **1**) or NH_3 (in **2**), Fig. 1 (panel b). The two six-membered rings of the ligated $P^{tBu}{}_2N^{Ph}{}_2$ ligand adopt a boat and chair configuration in both complexes. The pendant phenylamine group is in the boat conformation pointed towards the acetonitrile or NH_3 moiety with through-space N···N distance of 3.08 Å, and 3.04 Å, respectively. In **2**, an intramolecular hydrogen bonding interaction between the phenylamine and NH_3 is evident with a Ph-N···H–NH_2 distance of 2.46 Å.

After establishing NH_3 binding, complex **1** was examined as a precatalyst for the chemical oxidation of NH_3 to N_2 by using 2,4,6-tri-*tert*-butylphenoxyl radical ^{tBu}ArO$^\bullet$ as a

[a] Department of Chemistry and Biochemistry, Montana State University, Bozeman, MT 59717, USA. E-mail: michael.mock@montana.edu
[b] Department of Chemistry, Washington State University, Pullman, WA 99164, USA.
[c] Department of Chemistry, University of Wyoming, Laramie, WY 82071, USA.

† Electronic Supplementary Information (ESI) available: Experimental procedures, crystallographic details, additional spectroscopic data, and computational details. CCDC 2431617 (**1**), 2431618 (**2**). For ESI and crystallographic data in CIF or other electronic format see DOI: 10.1039/x0xx00000x

This journal is © The Royal Society of Chemistry 2025

Please do not adjust margins

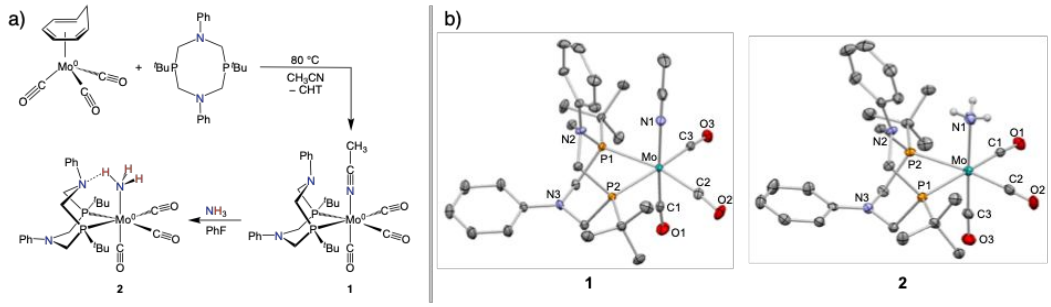

Fig. 1 (a) Synthesis of **1** and **2**. (b) molecular structures of **1** and **2**. Thermal ellipsoids are drawn at 50% probability. Co-crystallized PhF solvent in **2**, and hydrogen atoms are omitted for clarity except the H atoms of NH_3 for **2**. Selected bond distances (Å) and angles (°): (**1**) Mo–N1 = 2.230(3); Mo–P1 = 2.5152(8); Mo–P2 = 2.5210(8); Mo–C1 = 1.949(3); Mo–C2 = 1.984(3); Mo–C3 = 1.982(3); P1–Mo–P2 = 75.12(3); N1···N2 = 3.08. (**2**) Mo–N1 = 2.333(3); Mo–P1 = 2.5205(9); Mo–P2 = 2.5202(9); Mo–C1 = 1.963(4); Mo–C2 = 1.969(4); Mo–C3 = 1.934(3); P1–Mo–P2 = 75.17(3); N1···N2 = 3.04.

hydrogen atom acceptor.[17] The catalytic studies were performed in a similar manner to our previous studies using Ni complexes,[8] where **1** is reacted in 1,2-dimethoxyethane (DME) with 400−1200 equiv of $^{t\text{Bu}}$ArO$^{\bullet}$, and 1 atm of NH_3 for 24 h at room temperature. N_2 generated during catalysis was quantified via gas chromatography (GC) by sampling the headspace of the reaction vessel, see ESI†.

In an initial catalytic trial using 1.53 µmol **1** and 400 equiv $^{t\text{Bu}}$ArO$^{\bullet}$, 1.19 x 10^{-5} mol N_2 was quantified, corresponding to the formation of 7.8±0.1 equiv N_2 per Mo center. Increasing the catalyst and radical loading to 3.06 µmol and 1200 equiv, respectively, resulted in an insignificant change in total N_2 produced, leading to formation of 8.4±0.4 equiv of N_2 per Mo centre. Labelling experiments using $^{15}NH_3$ confirmed the N_2 formed in the catalytic reactions originates from NH_3. In a typical NMR tube experiment, 30 equiv $^{t\text{Bu}}$ArO$^{\bullet}$ and 12.3 µmol **1** were mixed in DME under 1 atm $^{15}NH_3$. After 24 h, the headspace gas was analysed by GC-MS revealing a prominent signal at *m/z* = 30, confirming the formation of $^{15}N_2$, see ESI†.

Next, we reacted **2^{15N}** with a stoichiometric amount of $^{t\text{Bu}}$ArO$^{\bullet}$ to identify possible Mo–$^{15}N_xH_y$ intermediates that are relevant to understanding the NH_3 oxidation mechanism en route to N_2 formation. A reaction of **2^{15N}** in THF-d_8 with 5 equiv $^{t\text{Bu}}$ArO$^{\bullet}$ in the *absence* of NH_3 was followed by ^{31}P NMR spectroscopy. Upon mixing, **2^{15N}** was consumed and $(CO)_4Mo(P^{tBu}{}_2N^{Ph}{}_2)$ (**Mo(CO)$_4$**) was identified by a resonance at 41 ppm in the ^{31}P NMR spectrum,[18] and a small amount of free $P^{tBu}{}_2N^{Ph}{}_2$ ligand. To verify this assignment, **Mo(CO)$_4$** was prepared independently from the addition of CO to **1**. In addition to N_2 generated in the catalytic reactions above, a small amount of free CO was noted in the GC analysis indicating CO dissociation from the Mo centre. Notably, the organic product 4-amino-2,4,6-tri-*tert*-butylcyclohexa-2,5-dien-1-one (H_2N-$^{t\text{Bu}}$ArO) was identified in this reaction by ^{1}H and ^{15}N NMR spectroscopy. The generation of H_2N-$^{t\text{Bu}}$ArO suggests that a putative Mo-NH_2 species, *fac*-$[(CO)_3Mo(P^{tBu}{}_2N^{Ph}{}_2)(NH_2)]$ (**3**) reacts with excess $^{t\text{Bu}}$ArO$^{\bullet}$ to form a C–N bond at the para position of the phenoxyl radical, Fig. 2. Bullock and co-workers described the analogous C–N coupling reaction using $(TMP)Ru(NH_3)_2$ (TMP = tetramesitylporphryin).[10d] In their Ru system, H_2N-$^{t\text{Bu}}$ArO was formed by the coupling of $^{t\text{Bu}}$ArO$^{\bullet}$ with a Ru–NH_2 intermediate generated by HAA of the parent $(TMP)Ru(NH_3)_2$ complex. $(TMP)Ru(NH_3)_2$ catalyzed the formation of ~600 equiv of H_2N-$^{t\text{Bu}}$ArO from NH_3 and $^{t\text{Bu}}$ArO$^{\bullet}$ and C–N coupling precluded catalytic N_2 formation.[13] To prevent C–N bond formation, Bullock and co-workers used 2,6-di-*tert*-butyl-4-tritylphenoxyl radical (^{trityl}ArO$^{\bullet}$) that contained a bulkier CPh_3 group at the para position of the aryl ring.[10d] While in the present Mo system catalytic NH_3 oxidation to N_2 is not completely inhibited using $^{t\text{Bu}}$ArO$^{\bullet}$, we postulated that using ^{trityl}ArO$^{\bullet}$ would enhance catalytic N_2 formation.

Repeating catalysis trials in triplicate under the identical reaction conditions as noted above, except using ^{trityl}ArO$^{\bullet}$, led to a significant enhancement of N_2 formation. A reaction of 1.53 µmol **1** with 400 equiv ^{trityl}ArO$^{\bullet}$ produced 3.7 x 10^{-5} mol N_2, corresponding to 24±5 equiv N_2 per Mo centre. Increasing the ^{trityl}ArO$^{\bullet}$ loading to 800 equiv produced up to 65 equiv N_2 per Mo centre; and with 1200 equiv ^{trityl}ArO$^{\bullet}$ up to 88 equiv N_2 per Mo centre was formed (ave. 77±15 equiv N_2 per Mo centre). Using the latter conditions, catalysis trials using **2** formed 54±9 equiv N_2 formed per Mo centre.

To probe if **3** exhibits sufficient unpaired spin-density to form a N–N bond in a bimolecular homocoupling process, Fig. 2[19] we attempted to identify *fac*-$[(CO)_3Mo(P^{tBu}{}_2N^{Ph}{}_2)]_2(\mu\text{-}^{15}N_2H_4)]$ (**4a**) or *fac*-$[(CO)_3Mo(P^{tBu}{}_2N^{Ph}{}_2)(^{15}N_2H_4)]$ (**4b**) starting from **2^{15N}**, Fig. 2. In an NMR tube experiment, treatment of **2^{15N}** in THF under Ar with 6 equiv ^{trityl}ArO$^{\bullet}$ *without* added NH_3 indicated only the presence of **2^{15N}** and **Mo(CO)$_4$** by ^{31}P NMR spectroscopy. **4a**/**4b** was not observed in this experiment; however, N_2 and CO were identified upon GC analysis of the gas in the headspace of the NMR tube. GC/MS analysis of the headspace gas generated in the reaction of a 1:1 mixture of **2** and **2^{15N}** in THF-d_8 with 10 equiv ^{trityl}ArO$^{\bullet}$ showed the nearly equal formation of $^{14}N^{15}N$ and $^{15}N^{15}N$ at *m/z* = 29 and *m/z* = 30, respectively, supporting the bimolecular homocoupling of **3** to form the N–N bond. We

This journal is © The Royal Society of Chemistry 2025

postulate that **4a** or **4b** generated in this experiment reacts with ^{trityl}ArO$^{\bullet}$ to form N_2, as described below.

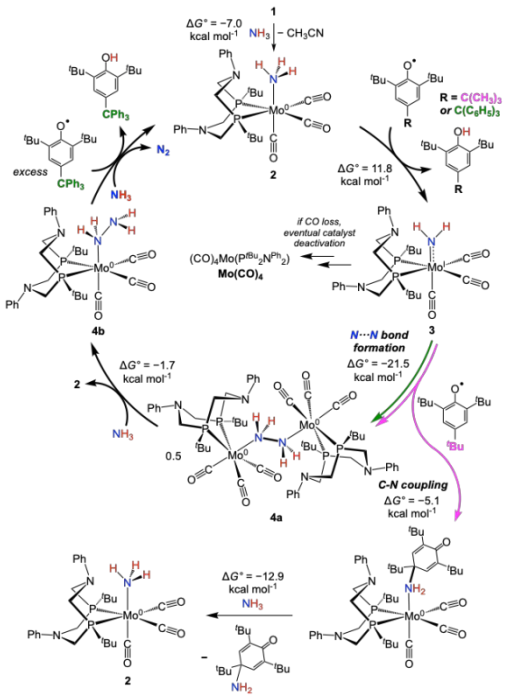

Fig. 2 Proposed mechanism for NH_3 oxidation to N_2 catalyzed by **2** as assessed by DFT calculations and the results of experiments probing reactivity of **1** and **2** with NH_3, N_2H_4, ^{tBu}ArO$^{\bullet}$ and ^{trityl}ArO$^{\bullet}$ Free energies calculated at 298 K (B3LYP-GD2/6-31G**// B3LYP-GD2/6-31G**/SMD-THF level of theory.)

In conjunction with the previously described experiments probing N–N bond formation, Density Functional Theory (DFT) calculations were performed to support a plausible catalytic cycle, Fig. 2. The Mo–L ligand exchange of CH_3CN for NH_3, converting **1** to **2**, was favourable (−7.0 kcal mol^{-1}) consistent with the experimental results. The bond dissociation free energy (BDFE) of the first NH_3 N–H bond in **2** was computed to be 86.3 kcal mol^{-1} indicating the H atom abstraction step is slightly unfavourable, $\Delta G°$ = 11.8 kcal mol^{-1} ($BDFE_{O\text{-}H}$ = 74.4 kcal mol^{-1} in THF[20] for ^{tBu}ArO–H; a similar value expected for ^{trityl}ArO–H). Experimentally, this step was achievable with a slight excess, ca. 6 equiv, of ^{trityl}ArO$^{\bullet}$. The HAA step from **3** to form an imido Mo–NH product was calculated to be appreciably unfavourable, $\Delta G°$ = 24.5 kcal mol^{-1} (see ESI†), suggesting this reaction is unlikely to occur using ^{R}ArO$^{\bullet}$. Supporting the homo- or heterocoupling reactivity of **3** to form **4a** or H_2N-^{tBu}ArO as noted above, calculations predicted that 43% unpaired spin-density resides on the N atom of the amido moiety in **3**, while 31% and 7% unpaired spin-density resides on Mo, and each of two CO ligands, respectively, see ESI†. N–N bond formation by a bimolecular homocoupling reaction was predicted to be an exergonic process, $\Delta G°$ = −21.5 kcal mol^{-1}. Based on these thermochemical data, we posit that the N–N bond forming step during catalysis proceeds through **4a** en route to N_2 formation. Intramolecular hydrogen bonding between the pendant amine and NH_2 groups noted in the computed structures of **3** and **4a/4b** may stabilize reaction intermediates formed during catalysis. The C–N bond forming step was computed to be thermodynamically less favourable, $\Delta G°$ = −5.1 kcal mol^{-1} than the homocoupling reaction. C–N bond formation is expected to be kinetically favoured in the presence of excess ^{tBu}ArO$^{\bullet}$. CO dissociation during catalysis likely generates **Mo(CO)$_4$** and leads to catalyst deactivation; however, this process may be sluggish in the presence of 1 atm of NH_3.

Lastly, we aimed to understand the fate of **4a** to discern the pathway in which N_2 is generated during catalysis. Treatment of **1** in THF-d_8 with 0.5 or 1 equiv of neat N_2H_4 under argon generated a mixture of **4a** and **4b** in a ~1:2 ratio, identified by ^{1}H, ^{31}P and ^{15}N NMR experiments, see ESI†. Experimentally we found exposure of the mixture of **4a/4b** with 1 atm NH_3 generates **4b** and **2**. This step was calculated to be close to thermoneutral, $\Delta G°$ = −1.7 kcal mol^{-1}. As a mixture of **4a/4b** could also be generated during catalysis, treatment with 10 equiv ^{trityl}ArO$^{\bullet}$ was performed to emulate reactivity under catalytic conditions. This reaction generated **2**, **Mo(CO)$_4$**, N_2 and NH_3 providing a plausible reaction path to N_2 formation via reaction with excess ^{trityl}ArO$^{\bullet}$. N_2H_4 dissociation from Mo and subsequent disproportionation in solution was also considered; however, the addition of neat N_2H_4 to a DME solution containing ^{trityl}ArO$^{\bullet}$ formed only N_2 and H_2 by GC analysis. Thus, the disproportionation of free N_2H_4 in the presence of excess ^{trityl}ArO$^{\bullet}$ led to distinctive selectivity for H_2 formation.[8] The absence of H_2 production in the catalytic reactions support N_2H_4 reacting as a metal-bound species.

In conclusion, we describe a Mo^0 complex activates NH_3 and catalyzes the oxidation of NH_3 to N_2. A key finding of this work is the notable reactivity of the Mo–NH_2 species (**3**) as a key intermediate. Catalytic NH_3 oxidation can be achieved using ^{tBu}ArO$^{\bullet}$ and ^{trityl}ArO$^{\bullet}$, with the latter radical generating up to 88 equiv N_2 per Mo centre, approaching the activity of chemocatalytic systems based on Ru using analogous conditions.[10d] Reactions using ^{tBu}ArO$^{\bullet}$ resulted in undesired C–N bond formation generating H_2N-^{tBu}ArO and only 8 equiv N_2 per Mo centre. **3** is proposed to form the N–N bond in catalysis by bimolecular homocoupling, generating a N_2H_4 complex **4a/4b**. The reaction of **4a/4b** with excess ^{trityl}ArO$^{\bullet}$ is postulated to generate N_2 in the last step of the catalytic cycle. This work guides current efforts in our laboratory that are focused on catalyzing NH_3 oxidation to N_2 using Mo complexes.

This material is based upon work supported by the National Science Foundation (NSF) under Grant No. CHE-1956161 and CHE-2247748. Support for MSU's NMR Center was provided by the NSF (Grant No. NSF-MRI: CHE-2018388 and DBI-1532078), the Murdock Charitable Trust Foundation (2015066:MNL), and MSU's office of the Vice President for Research and Economic Development. The authors gratefully acknowledge financial support for the X-ray diffractometer from the NSF (CHE 0619920) and an Institutional Development Award (IDeA) from the National Institute of General Medical Sciences of the National Institutes of Health (Grant # 2P20GM103432). Author contributions: R.J.B., investigation,

methodology, writing, editing; Z.M.H., computational investigation, writing; D.N.S., investigation, writing; N.A., investigation, writing; M.T.M, conceptualization, methodology, supervision, writing, editing, funding acquisition.

Data availability

The data supporting this article have been included as part of the Supplementary Information.

Conflicts of interest

There are no conflicts of interest to declare.

Notes and references

1. (a) F. Schüth, R. Palkovits, R. Schlögl and D. S. Su, *Energy Environ. Sci.*, 2012, **5**, 6278-6289; (b) S. Giddey, S. P. S. Badwal, C. Munnings and M. Dolan, *ACS Sustainable Chem. Eng.*, 2017, **5**, 10231-10239; (c) J. G. Chen, R. M. Crooks, L. C. Seefeldt, K. L. Bren, R. M. Bullock, M. Y. Darensbourg, P. L. Holland, B. Hoffman, M. J. Janik, A. K. Jones, M. G. Kanatzidis, P. King, K. M. Lancaster, S. V. Lymar, P. Pfromm, W. F. Schneider and R. R. Schrock, *Science*, 2018, **360**, No. eaar6611; (d) O. Elishav, B. Mosevitzky Lis, E. M. Miller, D. J. Arent, A. Valera-Medina, A. Grinberg Dana, G. E. Shter and G. S. Grader, *Chem. Rev.*, 2020, **120**, 5352-5436.
2. C. Smith, A. K. Hill and L. Torrente-Murciano, *Energy Environ. Sci.*, 2020, **13**, 331-344.
3. (a) N. V. Rees and R. G. Compton, *Energy Environ. Sci.*, 2011, **4**, 1255-1260; (b) R. Lan and S. Tao, *Front. Energy Res.*, 2014, **2**, 35.
4. (a) A. Kumar, V. Vibhu, J. M. Bassat, L. Nohl, L. G. J. de Haart, M. Bouvet and R. A. Eichel, *ChemElectroChem*, 2024, **11**, e202300845; (b) R. Lan, J. T. S. Irvine and S. Tao, *Int. J. Hydrogen Energy*, 2012, **37**, 1482-1494.
5. (a) D. N. Stephens and M. T. Mock, *Eur. J. Inorg. Chem.*, 2024, e202400039; (b) H.-Y. Liu, H. M. C. Lant, C. C. Cody, J. Jelušić, R. H. Crabtree and G. W. Brudvig, *ACS Catal.*, 2023, **13**, 4675-4682; (c) P. L. Dunn, B. J. Cook, S. I. Johnson, A. M. Appel and R. M. Bullock, *J. Am. Chem. Soc.*, 2020, **142**, 17845-17858.
6. H. Toda, K. Kuroki, R. Kanega, S. Kuriyama, K. Nakajima, Y. Himeda, K. Sakata and Y. Nishibayashi, *ChemPlusChem*, 2021, **86**, 1511-1516.
7. (a) M. D. Zott, P. Garrido-Barros and J. C. Peters, *ACS Catal.*, 2019, **9**, 10101-10108; (b) Y. Li, J. Y. Chen, Q. Miao, X. Yu, L. Feng, R. Z. Liao, S. Ye, C. H. Tung and W. Wang, *J. Am. Chem. Soc.*, 2022, **144**, 4365-4375; (c) M. D. Zott and J. C. Peters, *ACS Catal.*, 2023, **13**, 14052-14057; (d) L. Liu, S. I. Johnson, A. M. Appel and R. M. Bullock, *Angew. Chem. Int. Ed.*, 2024, **63**, e202402635; (e) M. D. Zott and J. C. Peters, *J. Am. Chem. Soc.*, 2021, **143**, 7612-7616; (f) M. E. Ahmed, R. J. Staples, T. R. Cundari and T. H. Warren, *J. Am. Chem. Soc.*, 2025, **147**, 6514-6522.
8. D. N. Stephens, R. K. Szilagyi, P. N. Roehling, N. Arulsamy and M. T. Mock, *Angew. Chem. Int. Ed.*, 2023, **62**, e202213462.
9. (a) M. E. Ahmed, M. Raghibi Boroujeni, P. Ghosh, C. Greene, S. Kundu, J. A. Bertke and T. H. Warren, *J. Am. Chem. Soc.*, 2022, **144**, 21136-21145; (b) H. Y. Liu, H. M. C. Lant, J. L. Troiano, G. Hu, B. Q. Mercado, R. H. Crabtree and G. W. Brudvig, *J. Am. Chem. Soc.*, 2022, **144**, 8449-8453.
10. (a) F. Habibzadeh, S. L. Miller, T. W. Hamann and M. R. Smith III, *Proc. Natl. Acad. Sci. U. S. A.*, 2019, **116**, 2849-2853; (b) P. Bhattacharya, Z. M. Heiden, G. M. Chambers, S. I. Johnson, R. M. Bullock and M. T. Mock, *Angew. Chem. Int. Ed.*, 2019, **58**, 11618-11624; (c) K. Nakajima, H. Toda, K. Sakata and Y. Nishibayashi, *Nat. Chem.*, 2019, **11**, 702-709; (d) P. L. Dunn, S. I. Johnson, W. Kaminsky and R. M. Bullock, *J. Am. Chem. Soc.*, 2020, **142**, 3361-3365; (e) M. J. Trenerry, C. M. Wallen, T. R. Brown, S. V. Park and J. F. Berry, *Nat. Chem.*, 2021, **13**, 1221-1227; (f) G. Chen, P. He, C. Liu, X.-F. Mo, J.-J. Wei, Z.-W. Chen, T. Cheng, L.-Z. Fu and X.-Y. Yi, *Nat. Cat.*, 2023, **6**, 949-958; (g) S. I. Jacob, A. Chakraborty, A. Chamas, R. Bock, L. Sepunaru and G. Ménard, *ACS Energy Lett.*, 2023, **8**, 3760-3766; (h) H. Toda, K. Kuroki, R. Kanega, T. Yano, T. Yoshikawa, S. Kuriyama, Y. Himeda, K. Sakata and Y. Nishibayashi, *Bull. Chem. Soc. Jpn.*, 2023, **96**, 980-988; (i) J. Holub, N. Vereshchuk, F. J. Sánchez-Baygual, M. Gil-Sepulcre, J. Benet-Buchholz and A. Llobet, *Inorg. Chem.*, 2021, **60**, 13929-13940; (j) H. Toda, R. Kanega, T. Yano, T. Yoshikawa, S. Kuriyama, Y. Himeda, K. Sakata and Y. Nishibayashi, *Chem. Lett.*, 2024, **53**, upae040; (k) B. Yuan, G. L. Tripodi, M. Derks, A. Y. Pereverzev, S. Zhou and J. Roithova, *Angew. Chem. Int. Ed.*, 2025, e202501617; (l) G. Chen, X. L. Ding, P. He, T. Cheng, Y. Chen, J. Lin, X. Zhang, S. Zhao, N. Qiao and X. Y. Yi, *Chem. Sci.*, 2025, **16**, 7573-7578; (m) J. Xie, T. Yang, L. Hong, H. Li, B. Li, Z. Guo, Y. Liu and T. C. Lau, *J. Am. Chem. Soc.*, 2025, **147**, 14211-14218; (n) C. Zhou, X. Zhang, S. Zhao, S.-D. Zhong, X.-L. Ding, S.-P. Yang, F. Pan, P. He and X.-Y. Yi, *ACS Catal.*, 2025, **15**, 3535-3545; (o) D. Guo, F. Liu, T. Liu, Z. Ji, X. Fan, B. Sun, P. Zhang, F. Li and F. Li, *ACS Catal.*, 2025, **15**, 8166-8173; (p) J. Li, X. Shi, F. Zhang, X. Lu, Y. Zhang, R. Liao and B. Zhang, *JACS Au*, 2025, **5**, 1812-1821.
11. (a) D. V. Yandulov and R. R. Schrock, *Science*, 2003, **301**, 76-78; (b) Y. Tanabe and Y. Nishibayashi, *Angew. Chem. Int. Ed.*, 2024, **63**, e202406404; (c) M. J. Chalkley, M. W. Drover and J. C. Peters, *Chem. Rev.*, 2020, **120**, 5582-5636.
12. (a) P. Bhattacharya, Z. M. Heiden, E. S. Wiedner, S. Raugei, N. A. Piro, W. S. Kassel, R. M. Bullock and M. T. Mock, *J. Am. Chem. Soc.*, 2017, **139**, 2916-2919; (b) C. C. Almquist, N. Removski, T. Rajeshkumar, B. S. Gelfand, L. Maron and W. E. Piers, *Angew. Chem. Int. Ed.*, 2022, **61**, e202203576; (c) M. J. Bezdek, S. Guo and P. J. Chirik, *Science*, 2016, **354**, 730-733; (d) S. I. Johnson, S. P. Heins, C. M. Klug, E. S. Wiedner, R. M. Bullock and S. Raugei, *Chem. Commun.*, 2019, **55**, 5083-5086.
13. C. C. Almquist, T. Rajeshkumar, H. Jayaweera, N. Removski, W. Zhou, B. S. Gelfand, L. Maron and W. E. Piers, *Chem. Sci.*, 2024, **15**, 5152-5162.
14. (a) L. S. Nogueira, P. Neves, A. C. Gomes, P. Lavrador, L. Cunha-Silva, A. A. Valente, I. S. Goncalves and M. Pillinger, *RSC Adv.*, 2018, **8**, 16294-16302; (b) D. Sieh, D. C. Lacy, J. C. Peters and C. P. Kubiak, *Chem. Eur. J.*, 2015, **21**, 8497-8503.
15. E. S. Wiedner, A. M. Appel, S. Raugei, W. J. Shaw and R. M. Bullock, *Chem. Rev.*, 2022, **122**, 12427-12474.
16. (a) B. J. Cook, S. I. Johnson, G. M. Chambers, W. Kaminsky and R. M. Bullock, *Chem. Commun.*, 2019, **55**, 14058-14061; (b) Z. Wang, S. I. Johnson, G. Wu and G. Ménard, *Inorg. Chem.*, 2021, **60**, 8242-8251.
17. V. W. Manner, T. F. Markle, J. H. Freudenthal, J. P. Roth and J. M. Mayer, *Chem. Commun.*, 2008, 256-258.
18. B. J. Elvers, C. Fischer and C. Schulzke, *Chem. Eur. J.*, 2024, **30**, e202304103.
19. N. Gu, P. Oyala and J. Peters, *Angew. Chem. Int. Ed.*, 2021, **60**, 4009-4013.
20. C. F. Wise, R. G. Agarwal and J. M. Mayer, *J. Am. Chem. Soc.*, 2020, **142**, 10681-10691.

This journal is © The Royal Society of Chemistry 2025

Data Availability Statement

The data supporting this article have been included as part of the Supplementary Information.